EDGE ARTICLE

Check for updates

FLP-type nitrile activation and cyclic ether ring-opening by halo-borane nonagermanide-cluster Lewis acid–base pairs†

Christoph Wallach,‡ Felix S. Geitner‡ and Thomas F. Fässler [ID] *

Even though homoatomic nine-atom germanium clusters are known for two decades, their chemical properties are still rarely investigated. We now discovered that Zintl ion main group-element clusters possess a reactive lone pair of electrons, and we show a new pathway to bind ligands with functional groups to the [Ge$_9$] cluster core through Ge–C bond formation. We report on the reactivity of [Ge$_9${Si(TMS)$_3$}$_2$]$^{2-}$ (TMS = trimethylsilyl) towards a series of Lewis acidic bromo-boranes. The reaction of [Ge$_9${Si(TMS)$_3$}$_2$]$^{2-}$ and DAB$^{o\text{-}tol}$–Br (DAB = 1,3,2-diazaborolidine; o-tol = 2-methylphenyl) resulted, depending on the reaction protocol, either in the formation of [Ge$_9${Si(TMS)$_3$}$_2$DAB$^{o\text{-}tol}$]$^-$ (**1a**) with direct Ge–B interactions, or in [Ge$_9${Si(TMS)$_3$}$_2$(CH$_2$)$_4$O–DAB$^{o\text{-}tol}$]$^-$ (**2a**) featuring a ring-opened thf moiety. Ring opening reactions occur for all bulkier DAB^R–Br [R: o-xyl (2,6-dimethylphenyl), Mes (2,4,6-trimethylphenyl), Dipp (2,6-diisopropylphenyl)], DAB$_{(II)}$^{Dipp}–Br and acyclic (^{i}Pr$_2$N)$_2$BBr without Ge–B bond formation as shown for the structural characterization of the ring-opened products of thf (**3**, **4**) and trimethylene oxide (**5**). In contrast to thf, the activation of CH$_3$CN requires the simultaneous presence of Lewis-acid and Lewis-basic reactants allowing the formation of [Ge$_9${Si(TMS)$_3$}$_2$CH$_3$C≡N–DAB^{Mes}]$^-$ (**6a**). Within the presented compounds, **3** and **4** show an unusual substitution pattern of the three ligands at the [Ge$_9$] core in the solid state. The [Ge$_9$] cluster/borane systems correspond to intermolecular frustrated Lewis pairs (FLPs), in which the [Ge$_9$] cluster with several lone pairs represents the Lewis base, and the borane is the Lewis acid.

Introduction

Main group element compounds and especially frustrated Lewis pairs (FLPs) have recently emerged in the field of small molecule activation. FLPs rely on a spatial separation of the Lewis-acidic and -basic sites preventing adduct formation and are known to interact with a plethora of different molecules including gasses, unsaturated systems or solvent molecules featuring polarizable bonds.[1–4] For the latter, as examples the main group assisted opening of cyclic ethers[5–9] or the reaction with nitriles,[10–15] which is often accompanied by ring formation, can be quoted.

Recently, the idea that transition-metal free [Ge$_9$] clusters might serve as Lewis base in Ge/boron based FLPs was put to

Department Chemie, Technische Universität München, Lichtenbergstraße 4, 85747 Garching b. München, Germany. E-mail: thomas.faessler@lrz.tum.de

front[16] and metal-functionalized [Ge$_9$]-Zintl clusters have been employed as homogeneous catalysts, in which the Ge atoms serve as a "support" for the catalytically active transition metal.[17] Homoatomic anionic nine-atom germanium clusters offer indeed a framework for a spatial arrangement of various functional groups and possess at least six Ge atoms with lone pairs pointing to the outside of the cage, resembling an overall six-fold Lewis base. Nonagermanide clusters are accessible in high yields and purity *via* fusion of stoichiometric amounts of K and Ge forming the Zintl phase K$_4$Ge$_9$ [18,19] containing discrete, extractable [Ge$_9$]$^{4-}$ anions.[20–23] In heterogeneous reactions organic main group element fragments are bound to the [Ge$_9$] core enhancing its solubility and stability. Thus, by treatment of solid K$_4$Ge$_9$ with stoichiometric amounts of an acetonitrile solution of chloro-tris(trimethylsilyl)silane the two- and three-fold silylated clusters [Ge$_9${Si(TMS)$_3$}$_2$]$^{2-}$ [24] and [Ge$_9${Si(TMS)$_3$}$_3$]$^-$ [25] are obtained, respectively. The transfer of this method to elusive [Si$_9$] clusters in the phase K$_{12}$Si$_{17}$ yielding [Si$_9${SiR$_3$}$_2$]$^{2-}$, [Si$_9${SiR$_3$}$_3$]$^-$ (R = TMS, ^{t}Bu$_2$H),[26,27] [Si$_9$H$_2$]$^{2-}$,[28] and [Si$_9$H]$^{3-}$ [29,30] shows the huge potential of this synthetic protocol using polar intermetallic compounds (Zintl phases) as precursors.

The addition of functional groups such as silyl fragments[24,31–35] to bare [Ge$_9$] allowed for a stabilization and

enhanced solubility of the cluster. Thus, mixed substituted clusters featuring various group 14 element fragments became accessible.[36–41] However, the attachment of phosphanyl-moieties[42–45] to [Ge$_9$] showed that the clusters can be decorated with more interesting Lewis basic functional groups. Similarly of interest is the addition of a ligand comprising an electron-deficient boranyl moiety by our group.

The boranyl functionalization of [Ge$_9$] clusters was achieved by the reaction of [Ge$_9$\{Si(TMS)$_3$\}$_2$]$^{2-}$ with the heterocyclic chloro-boranes DAB^R–Cl (R: Me, ^{i}Pr, o-tol; DAB: 1,3,2-diazaborolidine) yielding the anions [Ge$_9$\{Si(TMS)$_3$\}$_2$DAB^R]$^-$, thus introducing Lewis acidic moieties to the cluster. In fact, quantum chemical calculations corroborated the anion [Ge$_9$\{Si(TMS)$_3$\}$_2$BCy$_2$]$^-$ (Cy: cyclohexyl) to be an intramolecular frustrated Lewis acid–base pair (FLP), and its reactivity towards small molecules has been anticipated.[16] Within the system B/Ge, a bis-amido germylene-based Lewis acid/base-related pair is the only reported example, to the best of our knowledge. Since a Ge–B adduct is formed in the ground state, it does not correspond to a typical FLP, but nevertheless, a cleavage of the C=O bond of ketones or isocyanates has been observed.[46]

Triggered by the variety of reactions reported for FLP systems and on the basis of our recent achievements in combining boranes and [Ge$_9$] clusters, we now investigated the reactivity of [Ge$_9$\{Si(TMS)$_3$\}$_2$]$^{2-}$ as an appropriate Lewis base in combination with sterically hindered boron-based electrophiles, focusing on the reactivity towards molecules with polar groups. As boranes we applied the cyclic species DAB^R–Br (R: ^{i}Pr, o-tol, o-xyl, Mes, Dipp) and DAB(II)^{Dipp}–Br [(II): unsaturated backbone] as well as acyclic (^{i}Pr$_2$N)$_2$BBr, which (according to the acceptor number (AN) determined by the Gutmann–Beckett method) show an increased electrophilicity compared to the chloro-species used for the synthesis of the reported boranyl-functionalized clusters, thus featuring prerequisites for the formation of (reactive) FLPs.[16,47–49] Within the presented reactions the transition metal-free Zintl ions can be regarded as an active component in small molecule activation.

Results and discussion

Ring-opening of tetrahydrofuran

The reaction of equimolar amounts of [Ge$_9$\{Si(TMS)$_3$\}$_2$]$^{2-}$ and DAB^{o-tol}–Br in 1,4-dioxane selectively yields anionic [Ge$_9$\{Si(TMS)$_3$\}$_2$DAB^{o-tol}]$^-$ (**1a**). Besides the respective peak at m/z 1398.7 observed in the mass spectrum (Fig. S46†), the NMR data are congruent to the reaction product featuring a Ge–B bond as already reported for the reaction with DAB^{o-tol}–Cl (Fig. 1a).[16]

In thf as solvent for the reaction, the ^{1}H NMR spectrum of the solid residue shows the presence of two distinct species, which are identified as anions **1a** and [Ge$_9$\{Si(TMS)$_3$\}$_2$(CH$_2$)$_4$O–DAB^{o-tol}]$^-$, **2a** (δ = 0.24 ppm, thf-d_8) in a 60 : 40 ratio (Fig. 1b). This ratio changes to 15 : 85 performing the reaction at 35 °C. At higher temperature we observe formation of [Ge$_9$\{Si(TMS)$_3$\}$_3$]$^-$. To selectively yield anion **2a**, the bromo-borane is dissolved in thf in a first step and the bis-silylated cluster is added in a subsequent step leading to one single peak at m/z 1470.8
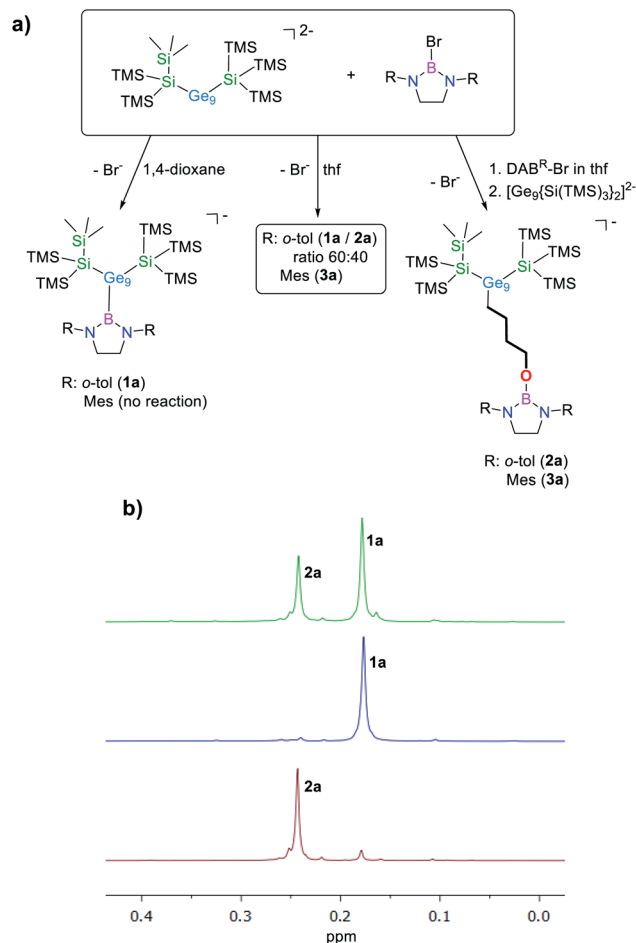

Fig. 1 (a) Reactivity of [Ge$_9$\{Si(TMS)$_3$\}$_2$]$^{2-}$ towards DAB^R–Br (R: o-tol, Mes) depending on the reaction conditions. (b) Selected areas of the ^{1}H NMR spectra of mixtures of **1a** and **2a** (top), pure **1a** (middle) and pure **2a** (bottom). All spectra were acquired in thf-d_8.

(Fig. S49†) in the ESI MS and the observation of one signal set in the ^{1}H NMR spectrum.

After redissolving the residues of analogous reactions performed in deuterated thf, an ESI mass peak at m/z 1478.8 (**2a-d_8**) is observed, indicative of the formation of the thf ring-opened species in which a –(CD$_2$)$_4$O– moiety is attached to the [Ge$_9$] cluster ion (Fig. S51†). It is noteworthy that pure **1a** does not react with thf under ring-opening. Using the sterically more hindered borane DAB^{Mes}–Br resulted in a complete conversion of the reactants to one single species within 3 h at room temperature in thf, as shown by ^{1}H NMR investigations. Recrystallization of the crude product from toluene at −40 °C yielded red crystals suitable for single crystal X-ray diffraction, which were identified as K[Ge$_9$\{Si(TMS)$_3$\}$_2$(CH$_2$)$_4$O-DAB^{Mes}], **3** (Fig. 2a and 3a).

The anion **3a** originates from thf ring-opening and insertion between the cluster and the boranyl ligand through Ge–C and B–O bond formation, respectively. The formation is confirmed by ESI MS spectra obtained from the intermediate solid products of the reaction using thf and thf-d_8 as solvents, resulting in
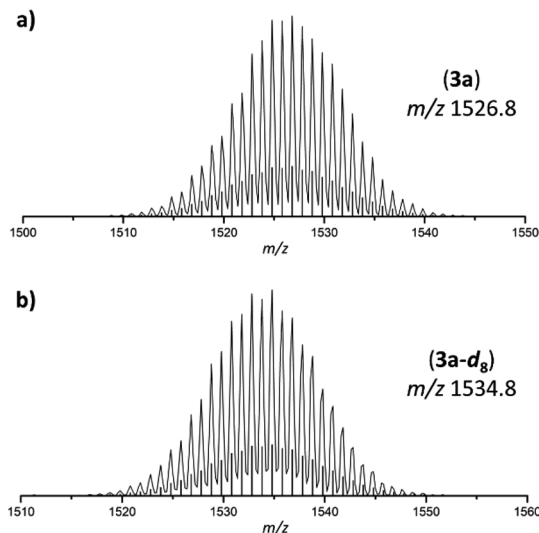
Fig. 2 Selected areas of ESI MS spectra (thf, negative-ion mode, 3500 V, 300 °C) of **3a** and **3a-d₈**. (a) Molecule peak of [Ge₉{Si(TMS)₃}₂(CH₂)₄O–DABᴹᵉˢ]⁻ (**3a**) at m/z 1526.8; (b) molecule peak of [Ge₉{Si(TMS)₃}₂(CD₂)₄O–DABᴹᵉˢ]⁻ (**3a-d₈**) at m/z 1534.8. Calculated isotope patterns are shown as black bars. Overview spectra are provided in the ESI.†

mass peaks at m/z 1526.8 (**3a**; Fig. 2a) and m/z 1534.8 (**3a-d₈**, Fig. 2b), respectively.

Similar reactions of [Ge₉{Si(TMS)₃}₂]²⁻ with DAB(ɪɪ)ᴰⁱᵖᵖ–Br yielded the respective anion [Ge₉{Si(TMS)₃}₂(CH₂)₄O–

DAB(ɪɪ)ᴰⁱᵖᵖ]⁻ (**4a**), with observed molecule peaks at m/z 1608.8 (**4a**, Fig. S57†) and m/z 1616.8 (**4a-d₈**, Fig. S59†). Full conversion of the reactants occurs upon stirring the reaction mixture for three weeks at 35 °C (at r. t. no reaction is observed at all due to the increased steric demand of the Dipp rest if compared to a Mes group).[50] A more convenient access to **4a** was found by heating a solution of DAB(ɪɪ)ᴰⁱᵖᵖ–Br in thf to 70 °C for 2 days, followed by the addition of [Ge₉{Si(TMS)₃}₂]²⁻. Compound **4**, K [Ge₉{Si(TMS)₃}₂(CH₂)₄O-DAB(ɪɪ)ᴰⁱᵖᵖ], was obtained by recrystallization of the crude material from toluene solution at −40 °C.

Compounds **3** and **4** crystallize in the triclinic space group $P\bar{1}$. In both compounds the bis-silylated clusters carry an additional ligand that comprises a ring-opened thf molecule which is further attached to the boranyl group through the oxygen atom. The [Ge₉] cluster cores are best described as distorted tricapped trigonal prisms with three different prims heights (Ge2–Ge4, Ge5–Ge6 and Ge7–Ge8) and thus C_S symmetry (Fig. 3a, b and d). All three substituents (one alkyl group and two silyl groups) form classical 2-center-2-electron (2c-2e) *exo*-bonds to single Ge vertices of the [Ge₉] cluster cores, with Ge–Ge, Ge–Si and Ge–C distances being in accordance with reported values (Table 1).[24,25,51–53] The alkyl group (–(CH₂)₄O–) and one of the silyl groups (Si1–Si4) are attached at Ge atoms capping the trigonal prism,[25,34,43,44] whereas the second silyl group (Si5–Si8) does not bind to the third capping atom Ge9, but to Ge5 instead, which is an atom of the trigonal prism base. This feature deviates from the typical substitution pattern in [Ge₉] clusters presented in Fig. 3e. Isomerization with
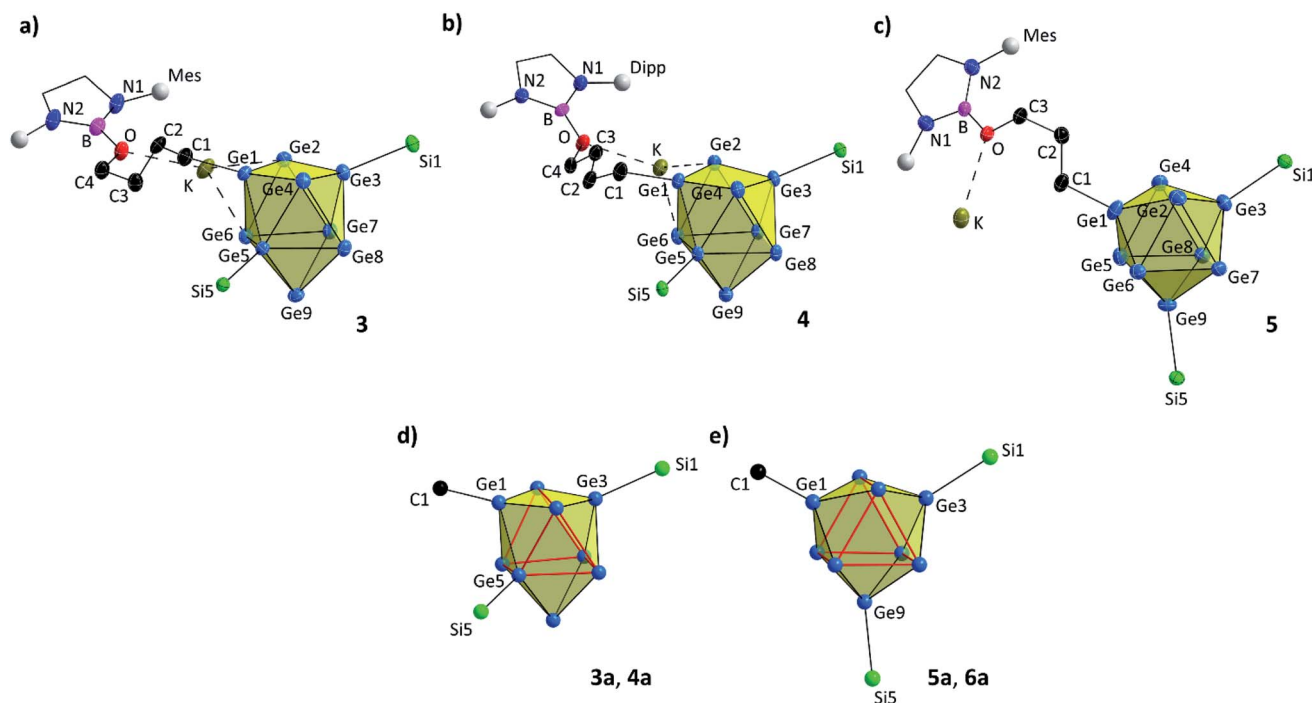

Fig. 3 Molecular structures of compounds **3–5** with uncommon (in **3** and **4**) and common (in **5**) substitution patterns of the [Ge₉] core. All ellipsoids are shown at a 50% probability level. For clarity protons, co-crystallized solvent molecules and TMS groups are omitted. Mes and Dipp fragments are shown as grey spheres, and carbon atoms of DAB and DAB(ɪɪ) moieties are presented as black wire sticks. (a) Molecular structure of **3** with –(CH₂)₄O– moiety; (b) molecular structure of **4** with –(CH₂)₄O– moiety; (c) molecular structure of **5** with –(CH₂)₃O– moiety; emphasis on (d) less common and (e) common substitution isomer of the [Ge₉] core in the anions **3a–6a** (trigonal prisms are indicated by bold red lines). Selected bond lengths and crystallographic data of **3–5** are presented in the ESI.†

Table 1 Selected bond lengths and prism heights h (both in Å) in compounds **3–6**. Additional bond lengths are presented in the ESI

	3	4	5	6
h_1	3.976(1)	3.918(1)	3.429(1)	3.370(1)
h_2	2.759(2)	2.815(2)	3.525(1)	3.663(1)
h_3	2.932(1)	2.934(1)	3.295(1)	3.201(1)
h_{long}/h_{short}	1.44	1.39	1.07	1.14
Ge–Ge$_{short}$	2.5038(8) (Ge1–Ge2)	2.5046(8) (Ge1–Ge2)	2.5031(9) (Ge6–Ge9)	2.5128(7) (Ge3–Ge7)
Ge–Ge$_{long}$	2.9322(8) (Ge7–Ge8)	2.9324(8) (Ge7–Ge8)	2.715(1) (Ge4–Ge8)	2.7396(7) (Ge4–Ge8)
Ge1–C1	1.995(5)	2.007(5)	1.984(6)	1.997(4)
Ge3–Si1	2.396(2)	2.392(2)	2.381(2)	2.369(1)
Ge5–Si5 or Ge9–Si5	2.395(2)	2.403(2)	2.383(2)	2.381(1)

respect to the ligand arrangement has been observed before.[54–56] However, NMR investigations of **3** in solution suggest a symmetrically decorated [Ge$_9$] cage with chemically and magnetically identical silyl groups (Fig. S32†). Even upon cooling of the NMR sample to −90 °C no splitting of the main signal could be observed, nevertheless a minor species (approx. 5%) showing a signal splitting could be monitored reaching its coalescence at 70 °C. Due to the low concentration we believe the latter signal is caused by an impurity. The asymmetric substitution in **3** and **4** could result from packing effects, and thus a rearrangement of the [Ge$_9$] cluster substituents or cluster vertex atoms might occur during crystallization.

The charge balancing potassium cations of **3a** and **4a** coordinate to two Ge vertices of the [Ge$_9$] unit and to the oxygen atom of the ring-opened ether (Fig. 3a and b). An influence of the K$^+$ cations on the course of the reaction was ruled out, since similar experiments, in which the cations were sequestered by 18-crown-6 or [2.2.2]-cryptand gave the same products. However, the coordination could play a role concerning which possible ligand arrangement at the [Ge$_9$] clusters is found in crystals of **3** and **4**.

These species resemble intermolecular frustrated Lewis pairs (FLPs) consisting of the bis-silylated [Ge$_9$] cluster (Lewis base) and the bromo-borane (Lewis acid). The formation of **3** and **4** reveals a new and very promising route to attach further ligands at the silylated [Ge$_9$] cluster. Currently, the formation of [Ge$_9$]–C bonds is limited to vinylation reactions, and a direct alkylation of the [Ge$_9$] cluster using alkyl-halides or acyl-chlorides[36,39] suffering either from low yields or limitation to neutral cluster species.[38]

The cleavage of endocyclic C–O bonds has been reported for boron based Lewis acids[57,58] as well as for non-electron-deficient boron subphthalocyanine, proposing the formation of a four-membered ring intermediate and subsequent σ-bond metathesis.[59,60] Therefore we tested the reactivity of the boranes DAB^R–Br towards thf in the absence of any cluster species. Indeed, NMR investigations (^{1}H, ^{11}B; Fig. S5 to S16†) of the residues obtained by stirring DAB^R–Br (R: o-tol; Mes) or DAB(II)^{Dipp}–Br in thf at room temperature or 70 °C, respectively, revealed thf ring-opening under formation of DAB^R–O–(CH$_2$)$_4$–Br. As observed for anions **2a** to **5a** the ^{11}B NMR shifts for the ring-opened species are only slightly up-field shifted if compared to the
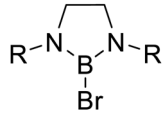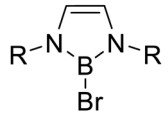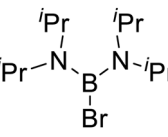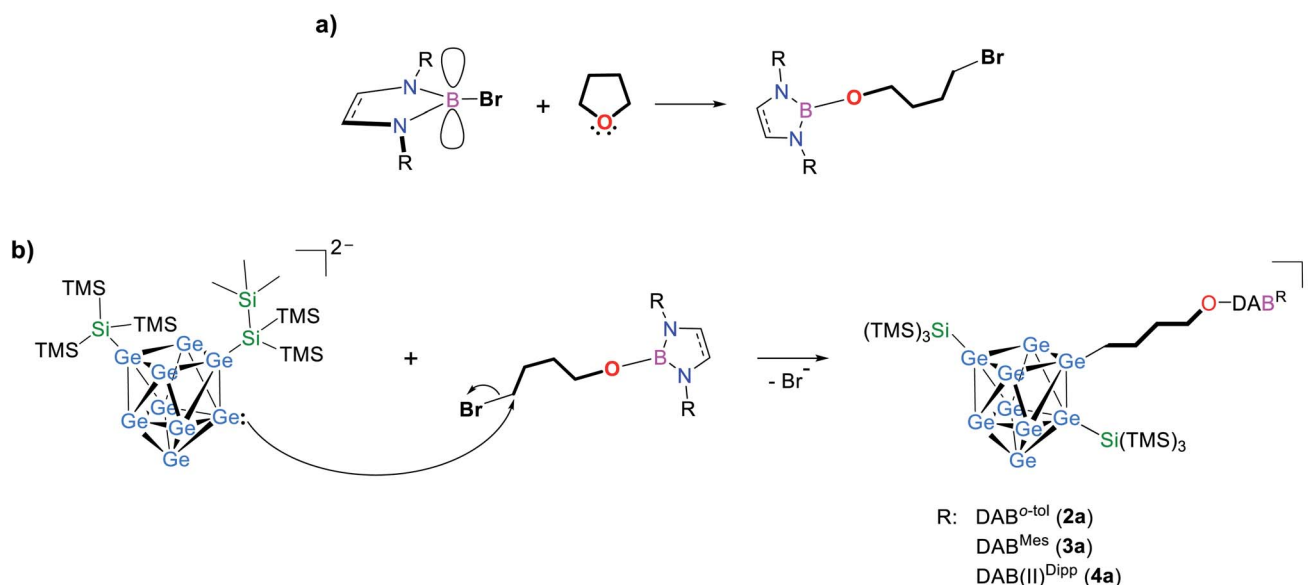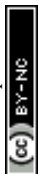

Scheme 1 Possible formation path for compounds **2–4** through (a) reaction of DAB^R–Br (R: o-tol, Mes) and DAB(II)^{Dipp}–Br with thf yielding ring-opened DAB^R–(CH$_2$)$_4$O–Br and (b) subsequent reaction with [Ge$_9${Si(TMS)$_3$}$_2$]$^{2-}$. Detailed reaction parameters are provided in the ESI.†

Table 2 Insertion of ring-opened ethers between $[Ge_9\{Si(TMS)_3\}_2]^{2-}$ and the respective borane, based on ESI MS studies (spectra presented in the ESI)

Reactant/solvent	(tetrahydrofuran)	(oxetane)
$R-N\overset{\overset{\displaystyle\frown}{B}}{\underset{Br}{}}N-R$	R: o-tol (2) o-xyl Mes (3) Dipp(4)	R: o-xyl Mes (5) Dipp
$R-N\overset{\overset{\displaystyle\frown}{B}}{\underset{Br}{}}N-R$	R: Dipp	R: Dipp
$^iPr-N\overset{^iPr\quad^iPr}{\underset{Br}{\overset{B}{N}}}N-^iPr$	Insertion observed	No insertion observed

DAB-reactants, indicating a similar chemical shielding of B. Upon the addition of $[Ge_9\{Si(TMS)_3\}_2]^{2-}$ species **2a** to **4a** are formed (Scheme 1), as shown by ESI MS experiments. Reactions with the less hindered DAB$^{o\text{-xyl}}$–Br, DAB^{Dipp}–Br (saturated backbone) and acyclic $(^iPr_2N)_2BBr$ led to the corresponding ring-opened products (Table 2), whereas in reactions with the analogous chloro-boranes DAB^R–Cl no ring opening of thf was observed (with and without $[Ge_9\{Si(TMS)_3\}_2]^{2-}$), which we assign to the lower Lewis acidity[47–49] of the chloro-borane, and Cl^- being a worse leaving group than Br^-.[61]

Ring-opening of trimethylene oxide

The reaction of $[Ge_9\{Si(TMS)_3\}_2]^{2-}$ with DAB^{Mes}–Br in tmo (trimethylene oxide) accordingly leads to the formation of $[Ge_9\{Si(TMS)_3\}_2(CH_2)_3O\text{–DAB}^{Mes}]^-$ (**5a**). Isolation of single crystals allowed the structural characterization and revealed the formation of $K[Ge_9\{Si(TMS)_3\}_2(CH_2)_3O\text{–DAB}^{Mes}]$ (**5**). ESI MS data of **5a** (m/z 1512.8, Fig. S61†), and NMR spectroscopic investigations corroborate the structure in solution. Compound **5** crystallizes in the triclinic space group $P\bar{1}$. The [Ge$_9$] cluster core can be best described as a tricapped trigonal prism with three different prims heights and C_S symmetry. All Ge–Ge, Ge–Si and Ge–C distances are in the range of the bond lengths observed in **3** and **4** (Table 1). In contrast to the asymmetric substitution pattern of the [Ge$_9$] cluster in **3** and **4**, the three substituents in **5** bind to the capping Ge atoms of the tricapped trigonal prismatic [Ge$_9$] core, as typically observed for tris-substituted [Ge$_9$] species (Fig. 3c and e).[25,34,43,44] Apparently, the slightly shorter alkyl chain changes the favoured structure in the solid state, and the potassium counter ion coordinates solely to the oxygen atom of the alkyl substituents and not to Ge vertices of the [Ge$_9$] cluster.

Reactions of $[Ge_9\{Si(TMS)_3\}_2]^{2-}$ with further bromo-boranes in tmo resulted in the formation of analogous species, which were characterized by ESI MS only (the spectra are shown in the ESI†). However, no selective ring-opening reaction could be observed for the reaction of tmo and various boranes DAB^R–Br, instead the formation of various unidentified products was observed in the NMR spectra. This indicates that a targeted opening of tmo is only feasible if Lewis basic and acidic moieties are simultaneously present. The results of these experiments show that the insertion of different cyclic ethers between the di-anionic cluster and several bromo-boranes corresponds to an easy route for Ge–C bond formation in [Ge$_9$] cluster chemistry (Table 2). Additional NMR spectra (^{1}H, ^{11}B, ^{13}C, ^{29}Si) of compounds **2** to **5** are provided in the ESI.†

Activation of CH$_3$CN

In contrast to thf the activation of CH$_3$CN requires the simultaneous presence of Lewis-acid and Lewis-basic reactants. A
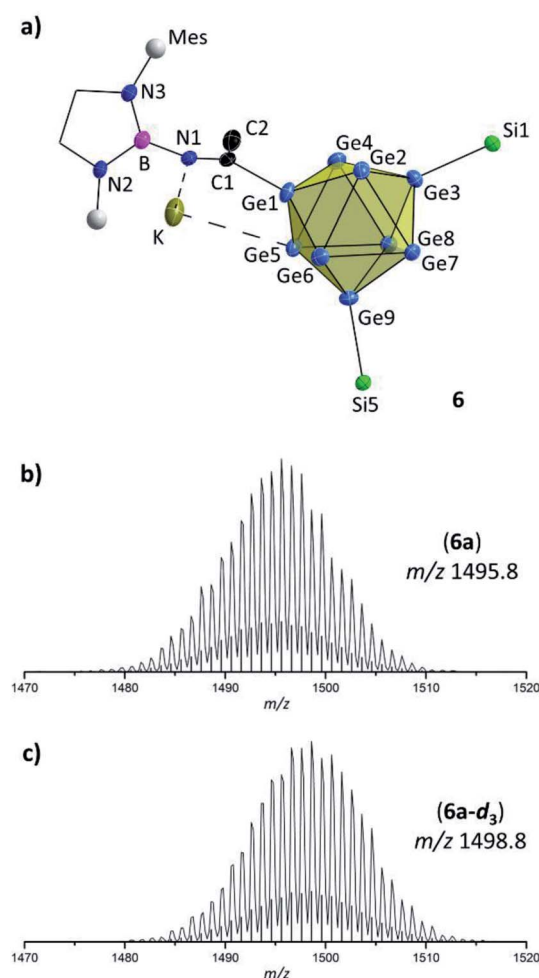

Fig. 4 (a) Molecular structure of compound **6** with –(CH$_3$)CN– moiety. All ellipsoids are shown at a 50% probability level. For clarity protons, co-crystallized solvent molecules and TMS groups are omitted. Mes fragments are indicated by grey spheres, and carbon atoms of the DAB moiety are presented as black wire sticks; (b) and (c) selected areas of ESI MS spectra (MeCN, negative-ion mode, 3500 V, 300 °C) of **6a** and **6a-d_3**; (b) molecule peak of $[Ge_9\{Si(TMS)_3\}_2CH_3C{=}N\text{–DAB}^{Mes}]^-$ (**6a**) at m/z 1495.8; (c) molecule peak of $[Ge_9\{Si(TMS)_3\}_2CD_3C{=}N\text{–DAB}^{Mes}]^-$ (**6a-d_3**) at m/z 1498.8. Calculated isotope patterns are shown as black bars. Overview spectra are given in the ESI.†
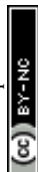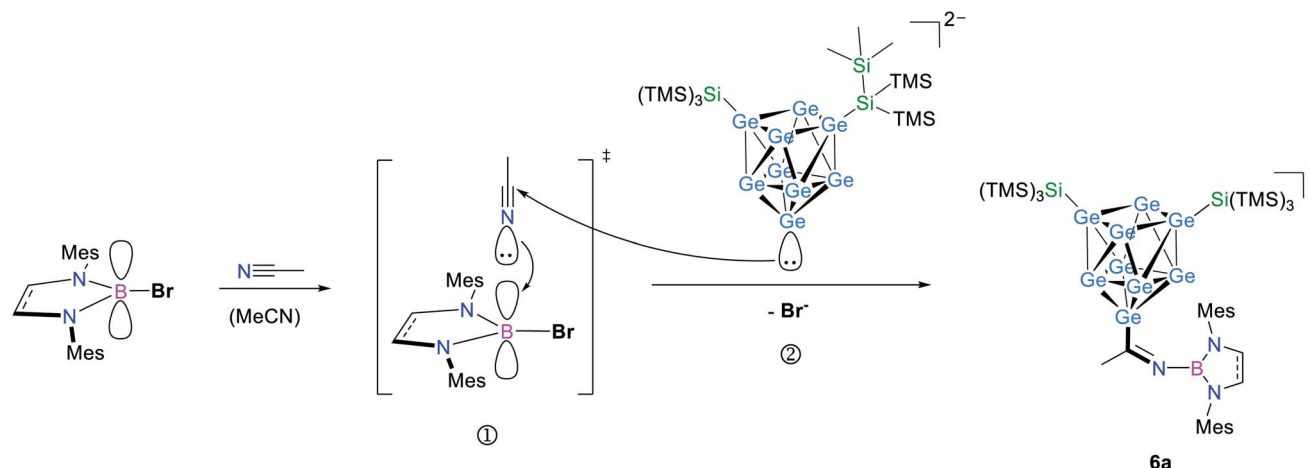
Scheme 2 Possible reaction path in analogy to the literature for the formation of **6a** through an intermediate activation of acetonitrile by the Lewis acid (①), subsequent attack of $[Ge_9\{Si(TMS)_3\}_2]^{2-}$ at the electrophilic C atom of the acetonitrile molecule (②) and product formation under cleavage of Br^-.[12,62]

reaction of the nitrile was only observed in the presence of $[Ge_9\{Si(TMS)_3\}_2]^{2-}$ and DAB^{Mes}–Br in acetonitrile solution, resulting in the anion $[Ge_9\{Si(TMS)_3\}_2CH_3C{=}N{-}DAB^{Mes}]^-$ (**6a**, Fig. 4a). By contrast, stirring acetonitrile solutions of DAB^{Mes}–Br at r. t. or at 70 °C overnight did not lead to any reaction, as shown by NMR spectroscopy (Fig. S19 and S20†). However, upon the addition of $[Ge_9\{Si(TMS)_3\}_2]^{2-}$, compound **6** is rapidly formed, as indicated by a shift of the silyl group protons from 0.16 ppm (bis-silylated [Ge$_9$] cluster) to 0.25 ppm in the ^1H NMR spectrum, a ^{11}B shift from 26 ppm to 18 ppm indicating an increased shielding of B and ESI MS investigations (**6a** at m/z 1495.8, **6a-d_3** at m/z 1498.8; Fig. 4b and c).

Hence, in contrast to the reactions with the cyclic ether thf, for which a ring opening reaction is already observed in the presence of the respective bromo-borane, MeCN insertion exclusively occurs in the presence of a Lewis acid–base pair (Scheme 2). Recrystallization of the crude product from toluene at room temperature yielded orange needles suitable for single crystal X-ray diffraction of $K[Ge_9\{Si(TMS)_3\}_2CH_3C{=}N{-}DAB^{Mes}]$ (**6**). Compound **6** crystallizes in the monoclinic space group $P2_1$. The [Ge$_9$] core has the shape of a tricapped trigonal prism with one prism height significantly elongated compared to the two others, resulting in C_{2v} symmetry (Table 1). As observed in **5**, the three substituents (one imine ligand and two silyl groups) bind to the capping Ge atoms of the cluster. The short bond d(C1–N1): 1.273(6) Å and the distorted trigonal planar coordination of C1 by Ge1, N1 and C2 [angles range between 114.2° (Ge1–C1–C2) and 124.4° (N1–C1–C2)] confirm the C=N double bond.[12] The potassium counter ion is coordinated by the imine nitrogen atom N1 and one Ge vertex atom (Ge5) of the [Ge$_9$] cluster core. Analogous ESI MS experiments for the boranes DAB^R–Br (R: o-xyl, Dipp), $DAB(II)^{Dipp}$–Br and $(^iPr_2N)_2B$–Br indicated insertion of the nitrile moiety between cluster and boranyl ligand only under simultaneous presence of both reactants. The results can be understood in terms of previous publications, which suggest a step-wise reaction path for the cyclo-addition of nitriles or azides to the intramolecular, geminal FLP $^tBu_2P{-}CH_2{-}BPh_2$.[12,62]

According to quantum chemical calculations the nitrile activation is initiated by the coordination of the terminal N atom of MeCN to the electrophilic boron center (intermediate), followed by the nucleophilic attack of the phosphorus' lone pair at the electrophilic C atom of the nitrile. In analogy, we assume that the $[Ge_9\{Si(TMS)_3\}_2]^{2-}$/DAB system forms a transition state (Scheme 2), and the reaction occurs according to a frustrated Lewis acid–base-type displacement reaction. These results are further corroborated by the observation that mixtures of $[Ge_9\{Si(TMS)_3\}_2]^{2-}$ and the acyclic chloro-borane $(^iPr_2N)_2B$–Cl readily react with MeCN under formation of $[Ge_9\{Si(TMS)_3\}CH_3C{=}N{-}B(N^iPr_2)_2]^-$ (chloro-boranes are less
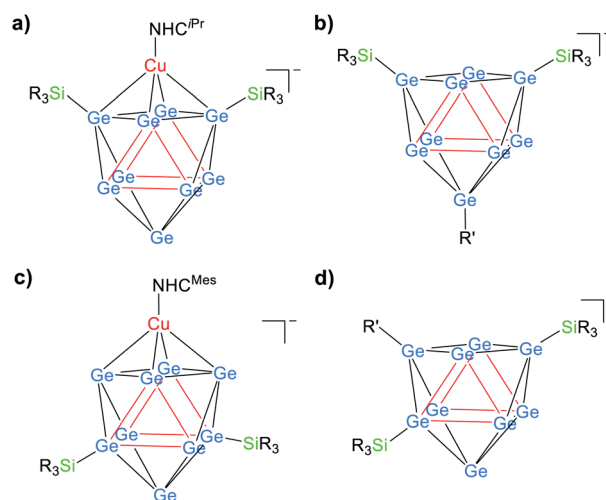
Fig. 5 Different substitution isomers of [Ge$_9$]. Common substitution pattern with (a) two *exo*-bonded silyl groups at Ge atoms capping the trigonal prism;[24,36,55] and (b) three ligands capping the trigonal prism.[25,34,35,43,44,65] Novel substitution isomers with (c) two silyl groups[55] and (d) three ligands binding to different cluster vertices (this manuscript). Trigonal prisms are indicated by red lines. NHC^{iPr}: 1,3-bis(iso-propyl)imidazolylidene; NHC^{Mes}: 1,3-bis(2,4,6-trimethylphenyl)imidazolylidene.

Lewis acidic than their bromo-congeners), whereas this cluster/borane pair does not open cyclic ethers. This contrasts the findings made for analogous mixtures of $[Ge_9\{Si(TMS)_3\}_2]^{2-}$ and cyclic DAB^R–Cl (R: o-tol, Mes), which do not react with MeCN. The difference in the reactivity of the respective cyclic and acyclic chloro-boranes can be explained by the significantly increased Lewis acidity of the acyclic $(^iPr_2N)_2B$–Cl compared to that of the cyclic DAB^R–Cl (R: o-tol, Mes) system. This is caused by a decreased electron density donation to the empty B p_z-type orbital due to the low barrier of the torsion about the B–N bond in the acyclic molecule.[63,64] Therefore, the Lewis acidity can be estimated to follow the sequence DAB^R–Br > $(N^iPr_2)_2$–BCl > DAB^R–Cl.

Conclusions

We reported on the reactivity of $[Ge_9\{Si(TMS)_3\}_2]^{2-}$ towards several bromo boranes DAB^R–Br. The reactions of the bis-silylated $[Ge_9]$ cluster with $DAB^{o\text{-tol}}$–Br reveal the tunability of this system, yielding either selectively the anion **1a** with direct Ge–B bond formation, or a participation of solvent molecules in the reaction. Anion **2a** is formed via the intermediate $DAB^{o\text{-tol}}$–$O(CH_2)_4$–Br, which subsequently reacts with $[Ge_9\{Si(TMS)_3\}_2]^{2-}$. Moreover, we found that boranes with sterically demanding ligands such as DAB^R–Br (R: o-xyl, Mes, Dipp), $DAB(II)^{Dipp}$–Br or $(^iPr_2N)_2B$–Br, which cannot bind to $[Ge_9\{Si(TMS)_3\}_2]^{2-}$, can also give species analogous to **2a** by ring opening of thf or tmo. By contrast, the insertion of CH_3CN takes place in analogy to a frustrated Lewis acid–base concept, since a reaction is observed only in the presence of both reactants $[Ge_9\{Si(TMS)_3\}_2]^{2-}$ (Lewis base) and DAB^R–Br (R: o-xyl, Mes, Dipp), $DAB(II)^{Dipp}$–Br or $(^iPr_2N)_2B$–Br (Lewis acid).

The structures of compounds **3** to **6** reveal another interesting aspect of the substitution pattern in spherical homoatomic germanium clusters: compounds **3** and **4** show an unusual substitution pattern of the $[Ge_9]$ cores in the solid state (Fig. 5), which is different from that in solution, indicating a rearrangement of the substituents upon crystallization.

To the best of our knowledge these systems are the first examples for intermolecular Ge/B frustrated Lewis acid–base pairs comprising nine-atom germanide clusters capable of reacting with small molecules. Currently, further investigations on the activation of small molecules by these germanide cluster/bromo-borane systems are carried out in our laboratories.

Author contributions

The experimental work was performed equally by C. W. and F. S. G. The manuscript was authored by C. W., F. S. G. and T. F. F.

Conflicts of interest

There are no conflicts to declare.

Acknowledgements

References

1 P. P. Power, *Nature*, 2010, **463**, 171.

2 D. W. Stephan, *Science*, 2016, **354**, aaf7229.

3 D. W. Stephan, *Acc. Chem. Res.*, 2015, **48**, 306.

4 D. W. Stephan and G. Erker, *Angew. Chem., Int. Ed.*, 2010, **49**, 46.

5 B. Birkmann, T. Voss, S. J. Geier, M. Ullrich, G. Kehr, G. Erker and D. W. Stephan, *Organometallics*, 2010, **29**, 5310.

6 S. Fantasia, J. M. Welch and A. Togni, *J. Org. Chem.*, 2010, **75**, 1779.

7 T. Krachko, E. Nicolas, A. W. Ehlers, M. Nieger and J. C. Slootweg, *Chem.–Eur. J.*, 2018, **24**, 12669.

8 G. C. Welch, J. D. Masuda and D. W. Stephan, *Inorg. Chem.*, 2006, **45**, 478.

9 G. Wittig and A. Rückert, *Justus Liebigs Ann. Chem.*, 1950, **566**, 101.

10 K. Samigullin, I. Georg, M. Bolte, H. W. Lerner and M. Wagner, *Chem.–Eur. J.*, 2016, **22**, 3478.

11 L. M. Elmer, G. Kehr, C. G. Daniliuc, M. Siedow, H. Eckert, M. Tesch, A. Studer, K. Williams, T. H. Warren and G. Erker, *Chem.–Eur. J.*, 2017, **23**, 6056.

12 E. R. Habraken, L. C. Mens, M. Nieger, M. Lutz, A. W. Ehlers and J. C. Slootweg, *Dalton Trans.*, 2017, **46**, 12284.

13 Z. Jian, G. Kehr, C. G. Daniliuc, B. Wibbeling and G. Erker, *Dalton Trans.*, 2017, **46**, 11715.

14 L. Keweloh, N. Aders, A. Hepp, D. Pleschka, E.-U. Würthwein and W. Uhl, *Dalton Trans.*, 2018, **47**, 8402.

15 J. Li, C. Mück-Lichtenfeld, C. G. Daniliuc, G. Kehr and G. Erker, *Angew. Chem., Int. Ed.*, 2020, **59**, 12477.

16 C. Wallach, F. S. Geitner, A. J. Karttunen and T. F. Fässler, *Angew. Chem., Int. Ed.*, 2021, **60**, 2648.

17 O. P. Townrow, C. Chung, S. A. Macgregor, A. S. Weller and J. M. Goicoechea, *J. Am. Chem. Soc.*, 2020, **142**, 18330.

18 S. Ponou and T. F. Fässler, *Z. Anorg. Allg. Chem.*, 2007, **633**, 393.

19 H. Von Schnering, M. Baitinger, U. Bolle, W. Carrillo-Cabrera, J. Curda, Y. Grin, F. Heinemann, J. Llanos, K. Peters and A. Schmeding, *Z. Anorg. Allg. Chem.*, 1997, **623**, 1037.

20 W. Carrillo-Cabrera, U. Aydemir, M. Somer, A. Kircali, T. F. Fässler and S. D. Hoffmann, *Z. Anorg. Allg. Chem.*, 2007, **633**, 1575.

21 C. Downie, J.-G. Mao and A. M. Guloy, *Inorg. Chem.*, 2001, **40**, 4721.

22 M. Somer, W. Carrillo-Cabrera, E. M. Peters, K. Peters and H. G. v. Schnering, *Z. Anorg. Allg. Chem.*, 1998, **624**, 1915.

23 C. Suchentrunk, J. Daniels, M. Somer, W. Carrillo-Cabrera and N. Korber, *Z. Naturforsch., B: J. Chem. Sci.*, 2005, **60**, 277.

24 O. Kysliak and A. Schnepf, *Dalton Trans.*, 2016, **45**, 2404.

25 F. Li and S. C. Sevov, *Inorg. Chem.*, 2012, **51**, 2706.

26 L. J. Schiegerl, A. J. Karttunen, W. Klein and T. F. Fässler, *Chem.–Eur. J.*, 2018, **24**, 19171.

27 L. J. Schiegerl, A. J. Karttunen, W. Klein and T. F. Fässler, *Chem. Sci.*, 2019, **10**, 9130.

28 L. J. Schiegerl, A. J. Karttunen, J. Tillmann, S. Geier, G. Raudaschl-Sieber, M. Waibel and T. F. Fässler, *Angew. Chem., Int. Ed.*, 2018, **57**, 12950.

29 C. Lorenz, F. Hastreiter, J. Hioe, N. Lokesh, S. Gärtner, N. Korber and R. M. Gschwind, *Angew. Chem., Int. Ed.*, 2018, **57**, 12956.

30 T. Henneberger, W. Klein and T. F. Fässler, *Z. Anorg. Allg. Chem.*, 2018, **644**, 1018.

31 K. Mayer, L. J. Schiegerl and T. F. Fässler, *Chem.–Eur. J.*, 2016, **22**, 18794.

32 O. Kysliak, C. Schrenk and A. Schnepf, *Inorg. Chem.*, 2015, **54**, 7083.

33 L. J. Schiegerl, F. S. Geitner, C. Fischer, W. Klein and T. F. Fässler, *Z. Anorg. Allg. Chem.*, 2016, **642**, 1419.

34 O. Kysliak, T. Kunz and A. Schnepf, *Eur. J. Inorg. Chem.*, 2017, **2017**, 805.

35 K. Mayer, L. Schiegerl, T. Kratky, S. Günther and T. Fässler, *Chem. Commun.*, 2017, **53**, 11798.

36 S. Frischhut, W. Klein and T. F. Fässler, *C. R. Chim.*, 2018, **21**, 932.

37 S. Frischhut and T. F. Fässler, *Dalton Trans.*, 2018, **47**, 3223.

38 F. Li and S. C. Sevov, *J. Am. Chem. Soc.*, 2014, **136**, 12056.

39 S. Frischhut, W. Klein, M. Drees and T. F. Fässler, *Chem.–Eur. J.*, 2018, **24**, 9009.

40 F. Li, A. Muñoz-Castro and S. C. Sevov, *Angew. Chem., Int. Ed.*, 2012, **51**, 8581.

41 O. Kysliak and A. Schnepf, *Z. Anorg. Allg. Chem.*, 2019, **645**, 335.

42 F. S. Geitner, W. Klein and T. F. Fässler, *Angew. Chem., Int. Ed.*, 2018, **57**, 14509.

43 F. S. Geitner, J. V. Dums and T. F. Fässler, *J. Am. Chem. Soc.*, 2017, **139**, 11933.

44 F. S. Geitner, C. Wallach and T. F. Fässler, *Chem.–Eur. J.*, 2018, **24**, 4103.

45 C. Wallach, F. S. Geitner, W. Klein and T. F. Fässler, *Chem.–Eur. J.*, 2019, **25**, 12349.

46 J. Li, B. Li, R. Liu, L. Jiang, H. Zhu, H. W. Roesky, S. Dutta, D. Koley, W. Liu and Q. Ye, *Chem.–Eur. J.*, 2016, **22**, 14499.

47 V. Gutmann, *Coord. Chem. Rev.*, 1976, **18**, 225.

48 M. A. Beckett, G. C. Strickland, J. R. Holland and K. S. Varma, *Polymer*, 1996, **37**, 4629.

49 I. B. Sivaev and V. I. Bregadze, *Coord. Chem. Rev.*, 2014, **270**, 75.

50 H. Clavier and S. P. Nolan, *Chem. Commun.*, 2010, **46**, 841.

51 A. Schnepf, *Angew. Chem., Int. Ed.*, 2003, **42**, 2624.

52 M. W. Hull and S. C. Sevov, *J. Am. Chem. Soc.*, 2009, **131**, 9026.

53 M. W. Hull, A. Ugrinov, I. Petrov and S. C. Sevov, *Inorg. Chem.*, 2007, **46**, 2704.

54 S. Frischhut, F. Kaiser, W. Klein, M. Drees, F. E. Kühn and T. F. Fässler, *Organometallics*, 2018, **37**, 4560.

55 F. S. Geitner and T. F. Fässler, *Inorg. Chem.*, 2020, **59**, 15218.

56 F. Li, A. Muñoz-Castro and S. C. Sevov, *Angew. Chem., Int. Ed.*, 2016, **55**, 8630.

57 H. C. Brown, P. V. Ramachandran and J. Chandrasekharan, *Heteroat. Chem.*, 1995, **6**, 117.

58 J. B. Heilmann, Y. Qin, F. Jäkle, H.-W. Lerner and M. Wagner, *Inorg. Chim. Acta*, 2006, **359**, 4802.

59 C. Bonnier and T. P. Bender, *Molecules*, 2015, **20**, 18237.

60 J. Guilleme, L. Martinez-Fernandez, D. Gonzalez-Rodriguez, I. Corral, M. Yanez and T. Torres, *J. Am. Chem. Soc.*, 2014, **136**, 14289.

61 M. B. Smith, *March's Advanced Organic Chemistry: Reactions, Mechanisms, and Structure*, John Wiley & Sons, Hoboken, New Jersey, Vol. 8, 2020, pp. 778–779.

62 D. H. Boom, A. R. Jupp, M. Nieger, A. W. Ehlers and J. C. Slootweg, *Chem.–Eur. J.*, 2019, **25**, 13299.

63 R. W. Alder, P. R. Allen, M. Murray and A. G. Orpen, *Angew. Chem., Int. Ed.*, 1996, **35**, 1121.

64 L. M. Slaughter, *ACS Catal.*, 2012, **2**, 1802.

65 O. Kysliak, C. Schrenk and A. Schnepf, *Inorg. Chem.*, 2017, **56**, 9693.